BBA - Molecular and Cell Biology of Lipids 1865 (2020) 158703

Contents lists available at ScienceDirect

BBA - Molecular and Cell Biology of Lipids

journal homepage: www.elsevier.com/locate/bbalip

Rab7 controls lipid droplet-phagosome association during mycobacterial infection

Natalia R. Roque[a], Silvia L. Lage[a], Roberta Navarro[a], Narayana Fazolini[a], Clarissa M. Maya-Monteiro[a], Jens Rietdorf[c], Rossana C.N. Melo[b], Heloisa D'Avila[b], Patricia T. Bozza[a,*]

[a] Laboratório de Imunofarmacologia, IOC, Fundação Oswaldo Cruz, Rio de Janeiro, 21045-900, RJ, Brazil
[b] Laboratório de Biologia Celular, Departamento de Biologia, Universidade Federal de Juiz de Fora, Juiz de Fora, 36036-330, MG, Brazil
[c] Centro de Desenvolvimento Tecnológico em Saúde, CDTS, IOC, Fundação Oswaldo Cruz, Rio de Janeiro, 21045-900, RJ, Brazil

ARTICLE INFO

Keywords:
LAM
Lipid droplet
Mycobacterium
Phagosomes
Rab
M. bovis BCG

ABSTRACT

Lipid droplets (LDs) are organelles that have multiple roles in inflammatory and infectious diseases. LD act as essential platforms for immunometabolic regulation, including as sites for lipid storage and metabolism, inflammatory lipid mediator production, and signaling pathway compartmentalization. Accumulating evidence indicates that intracellular pathogens may exploit host LDs as source of nutrients and as part of their strategy to promote immune evasion. Notably, numerous studies have demonstrated the interaction between LDs and pathogen-containing phagosomes. However, the mechanism involved in this phenomenon remains elusive. Here, we observed LDs and PLIN2 surrounding *M. bovis* BCG-containing phagosomes, which included observations of a bacillus cell surrounded by lipid content inside a phagosome and LAM from mycobacteria co-localizing with LDs; these results were suggestive of exchange of contents between these compartments. By using beads coated with *M.tb* lipids, we demonstrated that LD-phagosome associations are regulated through the mycobacterial cell wall components LAM and PIM. In addition, we demonstrated that Rab7 and RILP, but not Rab5, localizes to LDs of infected macrophages and observed the presence of Rab7 at the site of interaction with an infected phagosome. Moreover, treatment of macrophages with the Rab7 inhibitor CID1067700 significantly inhibited the association between LDs and LAM-coated beads. Altogether, our data demonstrate that LD-phagosome interactions are controlled by mycobacterial cell wall components and Rab7, which enables the exchange of contents between LDs and phagosomes and may represent a fundamental aspect of bacterial pathogenesis and immune evasion.

1. Introduction

Intracellular pathogens, including *Mycobacterium tuberculosis* (*Mtb*), *Mycobacterium leprae*, and the attenuated vaccine strain *M. bovis* BCG have evolved highly specialized mechanisms to manipulate host lipid metabolic pathways to obtain nutrients and persist within their host cells [1–5]. The formation of lipid droplets (LDs) during mycobacterial infections is a well-regulated phenomenon, and in addition to acting as a nutrient source, LDs also participate as an important escape mechanism for the pathogen [6–10]. Notably, host LDs are important sources of fatty acids and/or cholesterol for mycobacteria in vivo or in infected macrophages in culture [11,12]. LDs are sites of PGE_2 synthesis during *M. bovis* BCG infection, and this eicosanoid production could promote infection by deactivating macrophage functions [6,13–15]. Moreover, it has been demonstrated that *mycobacterium* can import and metabolize triacylglycerol (TAG) from host LDs [11,16]. Because mycobacteria harbor the genes *icl1* and *icl2*, the products of which are involved in the glyoxylate cycle, the utilization of LDs as a nutritional source appears to be a good strategy to survive inside the hostile environment of the phagosome [17].

Although it has been well documented that LDs can come into intimate contact with pathogen-containing phagosomes (reviewed in [18]), the mechanism by which this phenomenon occurs remains poorly understood. LDs were demonstrated in close proximity and even inside of phagosomes during bacterial [6–8,11,19]; fungi [20] and protozoan [21–24]; infection and this association may depend on specific combinations of both host and pathogen derived components. Indeed, LDs are recruited to the *M. leprae*–containing phagosomes in Schwann cell microtubules in a PI3K signaling–dependent, TLR2–independent manner [8]. *Toxoplasma* interacts and internalizes host LDs within

* Corresponding author.
E-mail address: pbozza@ioc.fiocruz.br (P.T. Bozza).

https://doi.org/10.1016/j.bbalip.2020.158703
Received 7 June 2019; Received in revised form 12 March 2020; Accepted 25 March 2020
Available online 27 March 2020
1388-1981/

parasitophorous vacuoles through parasite-secreted intravacuolar network [22].

A central feature of *M. tuberculosis* with respect to promoting survival inside macrophages is its capacity to prevent phagosomes that contain live bacteria from fusing with lysosomes [25,26]. The phagosome maturation process is dependent on a subset of proteins and their effectors. The emerging phagosome initially acquires the small GTPase Rab5 (an early endosome marker) and its effector, the early endosome antigen 1 (EEA-1), which then mediate the association with arriving endocytic vesicles [27]. Subsequently, the phagosome exchanges the Rab5 protein for the late endosome marker Rab7 [28–30] that, together with its effectors, mediates lysosome-phagosome fusion [31,32]. Among the effectors recruited to the phagosome by Rab7, Rab-interacting lysosomal protein (RILP) has an important role in linking GTP-Rab7 to the dynein-dynactin motor complex and to microtubules to mediate the centripetal movement toward phagosomes and lysosomes [32–34].

The ability of *M. bovis* and *M. tuberculosis* to retain Rab5 in the phagosome membranes and inhibit the exchange to Rab7 has been extensively investigated [35–37]. Several studies have described different but complementary mechanisms (most involving lipids from the mycobacterial cell wall or secreted proteins) to explain phagosomal maturation arrest caused by bacteria from the *M. tuberculosis* complex, including *M. bovis* BCG bacilli [36,38–41].

In this study, we propose novel mechanisms to explain LD interactions with mycobacteria-containing phagosomes. We provide evidence that the interaction between LDs and mycobacteria-containing phagosomes primarily occurs through the ability of bacterial cell wall components to "attract" LDs and through the accumulation of late endosome protein Rab7 and its effector RILP at LDs, which mediates LDs-phagosome interactions. Our results reveal new pathways in the complex process of host-mycobacteria interaction and provide a more detailed understanding of LD biology and its regulation upon mycobacterial infection, furthering our understanding of host-pathogen interactions and their impact on pathogenesis and the persistence of infections.

2. Material and methods

2.1. Animals and infection

C57BL/6 mice were obtained from the FIOCRUZ breeding unit. Animals were caged and maintained with free access to food and water at 22 to 24 °C and with a 12 h light/dark cycle at the FIOCRUZ animal facility. Animals weighing 20 to 25 g from both sexes were used. All protocols were approved by the Institutional animal welfare committee in agreement with the Brazilian National guidelines supported by CONCEA (Conselho Nacional de Controle em Experimentação Animal) under protocol CEUA/FIOCRUZ (L-002/08; L007/15).

2.2. Antibodies and reagents

Rabbit anti-Rab5A (cat# SC-309), anti-Rab7 (SC-10767), anti-RILP polyclonal IgG (cat# SC-98331)(Santa Cruz, Dallas, TX,) and anti-LAM polyclonal IgG (BEI Resources, NIAID, NIH, Fort Collins, CO, cat# NR-13821) were used for the fluorescence microscopy immunodetection studies. Irrelevant rabbit IgG was used at the same concentration as the primary antibodies (Jackson Immuno Research Laboratories, West Grove, PA, cat# 011-000-002). In addition, rabbit anti-Rab7 (10 μg/mL) (Santa Cruz Biotechnologies, Dallas, TX, cat# SC-10767) and guinea pig anti-PLIN2/ADRP (2 μg/mL) polyclonal IgG (Fitzgerald, Acton, MA, cat# 20R-AP002) were used for immunoelectron microscopy (immunoEM). The secondary antibodies used for Rab5 and Rab7 immunofluorescence assays were as follows: Cy3 donkey anti-rabbit (Jackson ImmunoResearch Laboratories, West Grove, PA, cat# 711-166-152); Alexa 546 goat anti-rabbit (Molecular probes, Eugene, OR, cat# A-11035) for RILP immunostaining; and Dylight 550 donkey anti-rabbit (Bethyl Laboratories, Montgomery, TX, cat# A140-107D3) for LAM. The secondary Ab used for immunoEM was an affinity-purified goat anti-rabbit or goat anti-guinea pig Fab fragment conjugated to 1.4-nm gold particles (Nanogold, Nanoprobes, Stony Brook, NY). The following reagents were also used in this study: LipidTOX™Red (Molecular Probes, Eugene, OR, cat# H34476), BODIPY®493/503, (Molecular Probes, Eugene, OR, cat# D3922), oleic acid (Sigma, Saint Louis, MO, cat# O1008), and the Ras superfamily of GTPases GTP/GDP binding antagonist CID 1067700 (Calbiochem, Burlington, MA, cat# 553326).

2.3. Pleurisy induced by BCG

Mice were intrapleurally (i.pl.) injected with labeled or unlabeled BCG (5×10^6 bacilli/cavity) in 100 μL of sterile saline. Control animals received an equal volume (100 μL) of sterile saline. After 24 h, the animals were euthanized by CO_2 inhalation, and their thoracic cavities were washed with 1 mL of ice-cold PBS. Pleural cells 0.1×10^6 cells were fixed in 3.7% formaldehyde for 10 min, washed, and then incubated with LipidTOX™Red or BODIPY®493/503 for 5 min for LD staining. Subsequently, the cells were rinsed with distilled water, mounted with VECTASHIELD mounting medium (Vector, Burlingame, CA, cat# H1000) and observed via fluorescence microscopy.

2.4. M. bovis BCG and mycobacterial lipids

The *M. bovis* BCG (Moreau strain) vaccine from Athaulpho de Paiva Foundation was resuspended in physiologic solution just before use or stored at 4 °C for one week from the day of dilution. Lipids from *Mycobacterium tuberculosis*, including lipoarabinomannan (LAM) and phosphatidylinositol mannosides (PIM) were obtained from BEI resources. PIM was conditioned in a chloroform/methanol solution (2:1) and LAM was conditioned in PBS and stored at −80 °C.

2.5. Preparation of LAM, PIM and LPS-coated beads

Latex beads (FluoresbritePolyFluor 570 Microspheres; Polysciences, Inc., Warrington, PA, cat# 24061-10) were prepared as described by Schlesinger et al. (35). Briefly, red fluorescent latex beads were centrifuged (10,000 ×*g*, 10 min) and washed twice with carbonate buffer 0.05 M (pH 9.6). LAM or PIM (50 μg) from *M. tuberculosis* and *M. bovis* BCG or Lipopolysaccharide (LPS) (50 μg) from *Escherichia coli* 0111:B4 Sigma-Aldrich (St. Louis, Mo) were added to the bead solution and incubated for 1 h at 37 °C. LAM, PIM, LPS or uncoated latex beads were incubated in a 1 mL reaction volume. Subsequently, the beads were washed twice with carbonate buffer and incubated in a 5% BSA solution in PBS for 2 h at 37 °C. The microspheres were then washed again and resuspended in 0.5% BSA. The beads were maintained at 4 °C and protected from light until the experiments were performed.

2.6. In vitro culture

2.6.1. Bone marrow macrophages (BMM)

BMM were generated from the marrow of femur bones from naive C57BL/6 mice. The BMM were differentiated in RPMI1640 (Gibco, Grand Island, NY, cat# 22400-089) supplemented with 10% fetal bovine serum (FBS), sodium pyruvate, 1% L-glutamine, 20% L929 cell-conditioned medium and 1% penicillin/streptomycin and cultured in a 5% CO_2 incubator for 7 days. Differentiated BMM (0.5×10^6 cells/ml) were plated onto cover slides within 24-wells culture plates and incubated overnight with RPMI 1640 cell culture medium containing 2% FBS and 2% penicillin. BMM were loaded with 50 μM of oleic acid for 24 h and then stimulated with LAM-, PIM-, LPS-coated beads or uncoated latex beads (10:1). The culture plate was centrifuged at 400 rpm for 4 min to pellet the beads onto the monolayers. After incubating for 2 h incubation at 37 °C, noninternalized beads were removed by

washing two times with sterile phosphate buffered saline (PBS), the medium was replaced, and cells were incubated 37 °C under a CO_2 atmosphere for 2 h. For the experiments using the Ras superfamily of GTPases GTP/GDP binding antagonist CID 1067700, after 2 h incubation at 37 °C, noninternalized beads were removed by washing two times with sterile phosphate buffered saline (PBS), which was followed by an incubation with or without CID1067700 (20 or 200 nM) for 2 h at 37 °C under a CO2 atmosphere. For enumeration the interactions, cells were fixed in 3.7% formaldehyde at room temperature (RT) for 10 min, and LDs were stained with BODIPY®493/503 (Molecular Probes, Eugene, OR, cat# D3922) for 5 min. The slides were mounted with VECTASHIELD mounting medium (Vector, Burlingame, CA) and examined by confocal microscopy. The percentage of latex beads that were observed in close apposition to LDs was quantified from 10 random images for each group (> 200 cells/group). The distance between latex beads and LDs was evaluated by analyzing the confocal images using Fiji/ImageJ. Cell viability was assessed by trypan blue exclusion at the end of each experiment and was always > 90%.

2.7. Fluorescently labeled BCG

BCG was labeled using a Live/Dead BacLight bacterial viability kit (Molecular Probes, Eugene, OR) prior to infection following the manufacturer's instructions. The BCG suspension was incubated with 1.5 μL of component A (Syto 9) for 15 min in the dark, and the cells were subsequently washed twice and resuspended in PBS.

2.8. Rab5, Rab7, RILP and LAM immunolocalization

Macrophages obtained from BCG-infected animals were cytocentrifuged and fixed in 3.0% formaldehyde for 10 min, after which they were washed and permeabilized with 0.1% Triton for 20 min at RT. Subsequently, slides were blocked with 1% normal goat serum for 1 h and then washed and incubated with rabbit polyclonal anti-Rab5, rabbit polyclonal anti-Rab7, rabbit polyclonal anti-RILP or rabbit polyclonal anti-LAM diluted in PBS for 1 h at RT. As a control, rabbit IgG at same concentration was used in place of the primary antibody. Prior to the primary antibody incubation, cells were washed three times with PBS for 7 min each and then incubated with the secondary antibodies Cy3 donkey anti-rabbit, Alexa 546 goat anti-rabbit, and Dylight 550 donkey anti-rabbit for 1 h at RT. After three washes for 7 min each, the LDs were labeled with BODIPY® (1:500) for 5 min. Subsequently, the cells were washed, and the slides were mounted using VECTASHIELD mounting medium. The slides were examined via fluorescence (Rab5 and Rab7) or confocal microscopy (RILP and LAM).

2.9. Electron microscopy for PLIN2/ADRP and Rab7

For immunoEM, pleural cells from the control and infected animals (5×10^6 of BCG/cavity for 24 h) were fixed in a mixture of freshly prepared aldehydes (1% paraformaldehyde and 1% glutaraldehyde) in 0.1 M phosphate buffer (pH 7.3) overnight at 4 °C as previously described. The cells were then washed in the same buffer and embedded in molten 2% agar. Agar pellets were immersed in 30% sucrose in PBS overnight at 4 °C, embedded in OCT compound (Miles, Elkhart, IN), and then stored in liquid nitrogen at −180 °C for subsequent use.

As previously described [42,43], pre-embedding immunolabeling was performed prior to standard EM processing (postfixation, dehydration, infiltration, resin embedding and resin sectioning). All labeling steps were performed at RT as previously described [44] as follows: a) one wash in 0.02 M PBS (pH 7.6) for 5 min; (b) immersion in 50 mM glycine in 0.02 MPBS (pH 7.4) for 10 min; (c) incubation in a mixture of PBS and BSA (PBS-BSA buffer; 0.02 M PBS plus 1% BSA) containing 0.1% gelatin for 20 min followed by an incubation in PBS-BSA plus 10% normal goat serum (NGS) for 30 min (this step is crucial to block nonspecific antibody binding sites); (d) incubation with the primary antibody for 1 h; (e) blocking with PBS-BSA plus NGS for 30 min; (f) incubation with the an HQ secondary antibody for 1 h; (g) washing in PBS-BSA (three times of 5 min each); (h) post fixation in 1% glutaraldehyde for 10 min; (i) five washes with distilled water; (j) incubation with an HQ silver enhancement solution in a darkroom according to the manufacturer's instructions (Nanoprobes) for 10 min (this step enables the nucleation of silver ions around gold particles that precipitate as silver metal and grow in size to facilitate TEM observations); (k) three washes in distilled water; (l) immersion in freshly prepared 5% sodium thiosulfate for 5 min; (m) post fixation with 1% osmium tetroxide in distilled water for 10 min; (n) staining with 2% uranyl acetate in distilled water for 5 min; (o) embedding in Eponate 12 resin (Ted Pella Inc., Redding, CA); (p) after polymerization at 60 °C for 16 h, embedding was performed by inverting eponate-filled plastic capsules over the slide-attached tissue sections; and (q) separation of eponate blocks from glass slides by a brief immersion in liquid nitrogen. Thin sections were cut using a diamond knife on an ultramicrotome (Leica, Bannockburn, IL). Sections were mounted onto uncoated 200-mesh copper grids (Ted Pella) before staining with lead citrate and viewing with a CM 10 transmission electron microscope (Philips, Eindhoven, The Netherlands) at 60 kV. Two controls were used where (1) the primary antibody was replaced with an irrelevant antibody, and (2) the primary antibody was omitted. Electron micrographs were randomly taken at different magnifications to study the entire cell profile and subcellular features. A total of 88 electron micrographs for conventional TEM, 17 electron micrographs for Rab7 labeling, 56 electron micrographs for ADRP/PLIN2 labeling and 22 electron micrographs for control IgG were evaluated.

2.10. Image acquisition

The images were obtained using an Olympus IX81 fluorescence microscope equipped with a Plan Apo 100× 1.4 Ph3 objective (Olympus Optical) and a CoolSNAP-Pro CF digital camera with Image-Pro Plus version 4.5.1.3 (Media Cybernetics). Confocal images were obtained using an Olympus FV1000 microscope and FV10-ASW 4.1. The images were edited using Adobe Photoshop CS5 version 12.0 (Adobe Systems). Coloc2 plugin of Fiji were used to determine the Manders' colocalization coefficients.

2.11. Statistical analysis

The results were statistically analyzed using Prism 6.01 (GraphPad software, San Diego, CA) and are expressed as the mean values ± SEM. Paired two-tailed *t*-test was used to evaluate the significance of two groups. One-way ANOVA in Tukey's multiple comparison test was used to evaluate the significance of more than two groups that were all normally distributed. A value of $P \leq 0.05$ was considered statistically significant.

3. Results

3.1. M. bovis BCG induces LD-phagosome interactions and lipid exchange during infection

The apposition between LDs and phagosomes during mycobacterial infections have been extensively described, including the transfer of lipids from LDs to mycobacteria [6,7,45–47]. With the goal of examining the mechanisms involved in LD-phagosome association, we first validated the association in our model of C57/BL6 mice were intrapleurally infected with Syto9-labeled BCG for 24 h. Using confocal microscopy, we observed pleural cells infected with BCG (green channel) surrounded by LDs (red channel) labeled with the probe LipidTox Red (Fig. 1A). In parallel, pleural cells from infected animals were fixed and immunolabeled for ultrastructural detection of perilipin-2/adipose differentiation-related protein (PLIN2/ADRP) using a

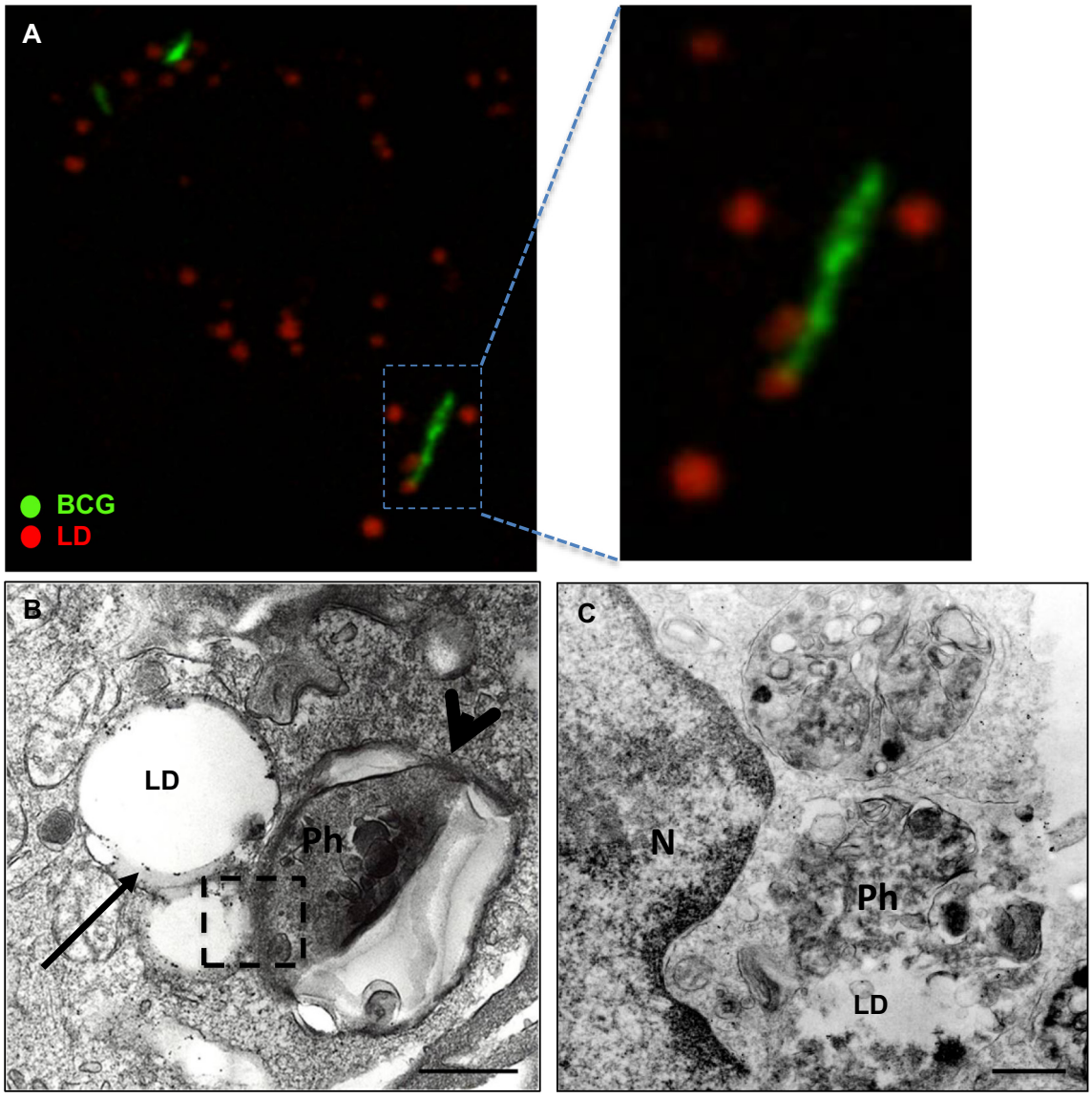

Fig. 1. Interaction between lipid droplets (LDs) and infected phagosomes. C57/Bl6 mice were i.pl. infected with BCG (5×10^6 CFU/cavity) for analyses of pleural macrophages after 24 h. (A) Spatial organization of LDs labeled with LipidTox red (red) around Syto9 labeled-BCG (green) by confocal microscopy. (B) Immunogold labeled LDs for PLIN2 (arrow), phagosome (Ph, arrowhead), LD-phagosome association (detailed) by Transmission Electron Microscopy. (C) A LD in contact with a phagosome in which purified IgG was used as control for PLIN2 labeling, N, nucleus. Bars: 10 μm (A) and 1 μm (B, C). (A) Data are representative from one of at least three independent experiments. (B and C) Representative images from two independent experiments.

methodology that enables superior antigen/morphology preservation and optimal antibody access to membrane microdomains for conventional transmission electron microscopy (TEM) [44,48]. The interaction between PLIN2/ADRP-positive LDs and phagosomes were observed after 24 h of infection, which was consistent with previous observations [6,7] (Fig. 1B and Fig. S1). As control for PLIN2 labeling we used a negative control in which the primary antibody was replaced by an irrelevant IgG (Fig. 1C). Interestingly, quantitative analysis of LD morphology by conventional TEM revealed that 71.87% of all LDs exhibited morphological changes (irregular surface) in infected group compared to only 8.4% in control group (22 = LDs; n = 26 cells). Most LDs showing irregular surface were in close apposition with or within phagosomes (Fig. 1C, Fig. S2 A–C). Morphological analyses by TEM revealed 59.45% of phagosome containing BCG or amorphous material embedded in lipids in infected macrophages, suggesting the occurrence of fusion between those organelles (Fig. 2A and Ai). The fusion of LDs with other organelles in the control group was not observed.

To further characterize the association of LDs with phagosome containing mycobacteria, we performed immunolocalization of the mycobacteria cell wall glycolipid LAM (red channel) aiming at determining mycobacteria location in the macrophages by using confocal microscopy. Of note, beside the typical bacilli shaped staining obtained with anti-LAM Ab (arrowhead, Fig. 2B and C), we also observed a ring-shaped LAM staining (Fig. 2B). As observed in Fig. 2B, the ring-shaped staining for LAM surround the BODIPY-labeled LDs (Amount of signal overlap between LAM (M1) and BODIPY (M2) channels determined by Manders' colocalization coefficients were 0.755 (M1) and 0.552 (M2)), suggestive of trafficking of BCG-derived LAM to LDs. Further studies are needed to better characterize the potential trafficking of bacterial lipids to LDs. Altogether, these results suggest the bidirectional exchange of lipids between LDs and phagosomes.

3.2. Mycobacterial cell wall components are involved in LD-phagosome interactions

Mycobacterial cell wall components have been described as having

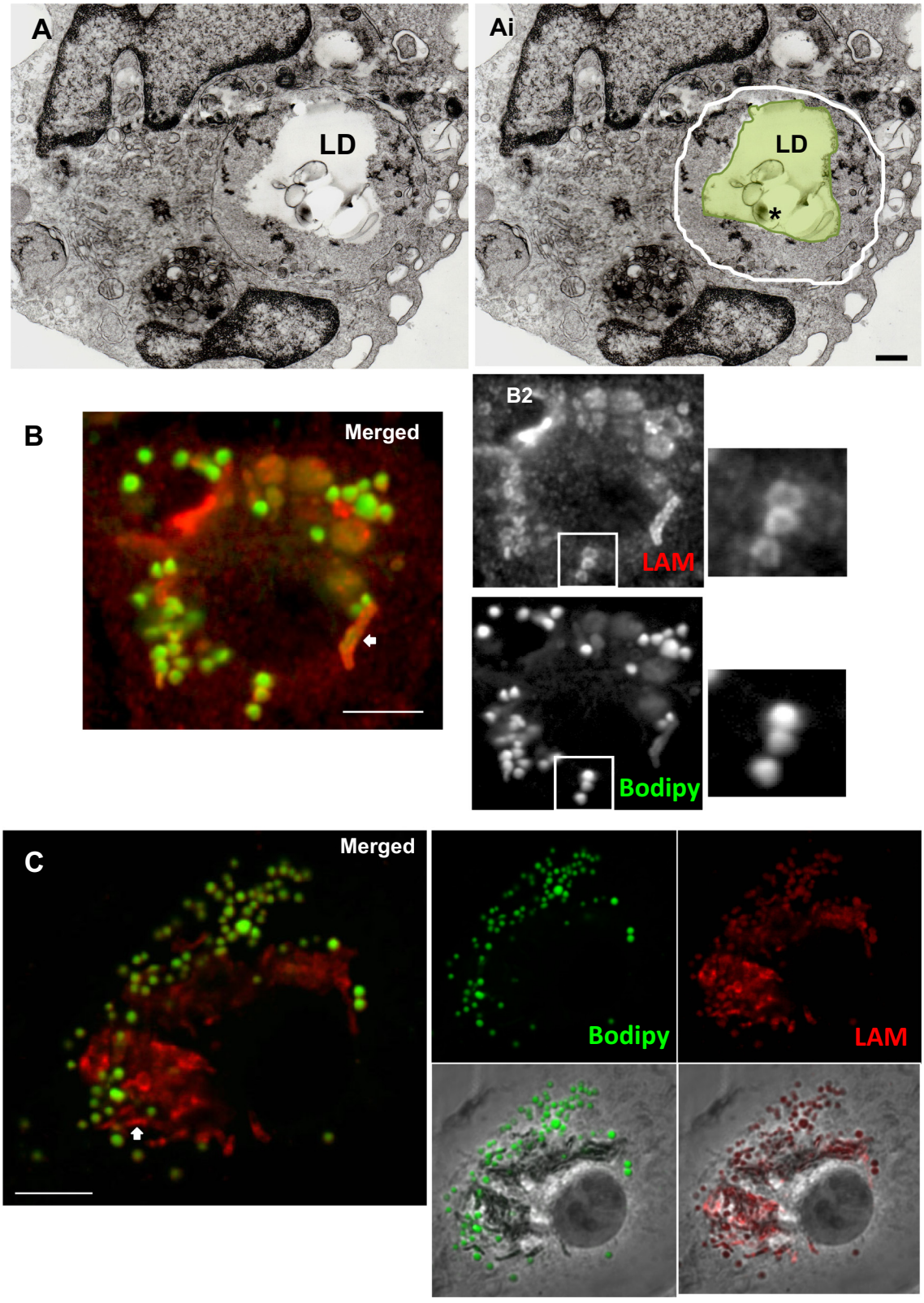

Fig. 2. Exchange of lipids between phagosomes and lipid droplets (LDs). C57/Bl6 mice were i.pl. infected with BCG (5×10^6 CFU/cavity) for analyses of pleural macrophages after 24 h. (A) TEM shows an infected phagosome filled with lipid content. In Ai, the phagosome (white line) containing lipids (in green) and bacteria (*) were highlighted. (B and C) Bone marrow macrophages were infected with BCG for 24 h. Immunofluorescence showed LAM (red) colocalized with BODIPY-labeled LD (green) in addition to bacteria labelling (arrowhead). (C) widefield plus red and green channel. Bar: 1 μm (Ai) and 5 μm (B, C). (A) Data is a representative image of a total of 96 LDs analyzed in 2 independent experiments (B) Data are representative confocal image from at least two independent experiments.

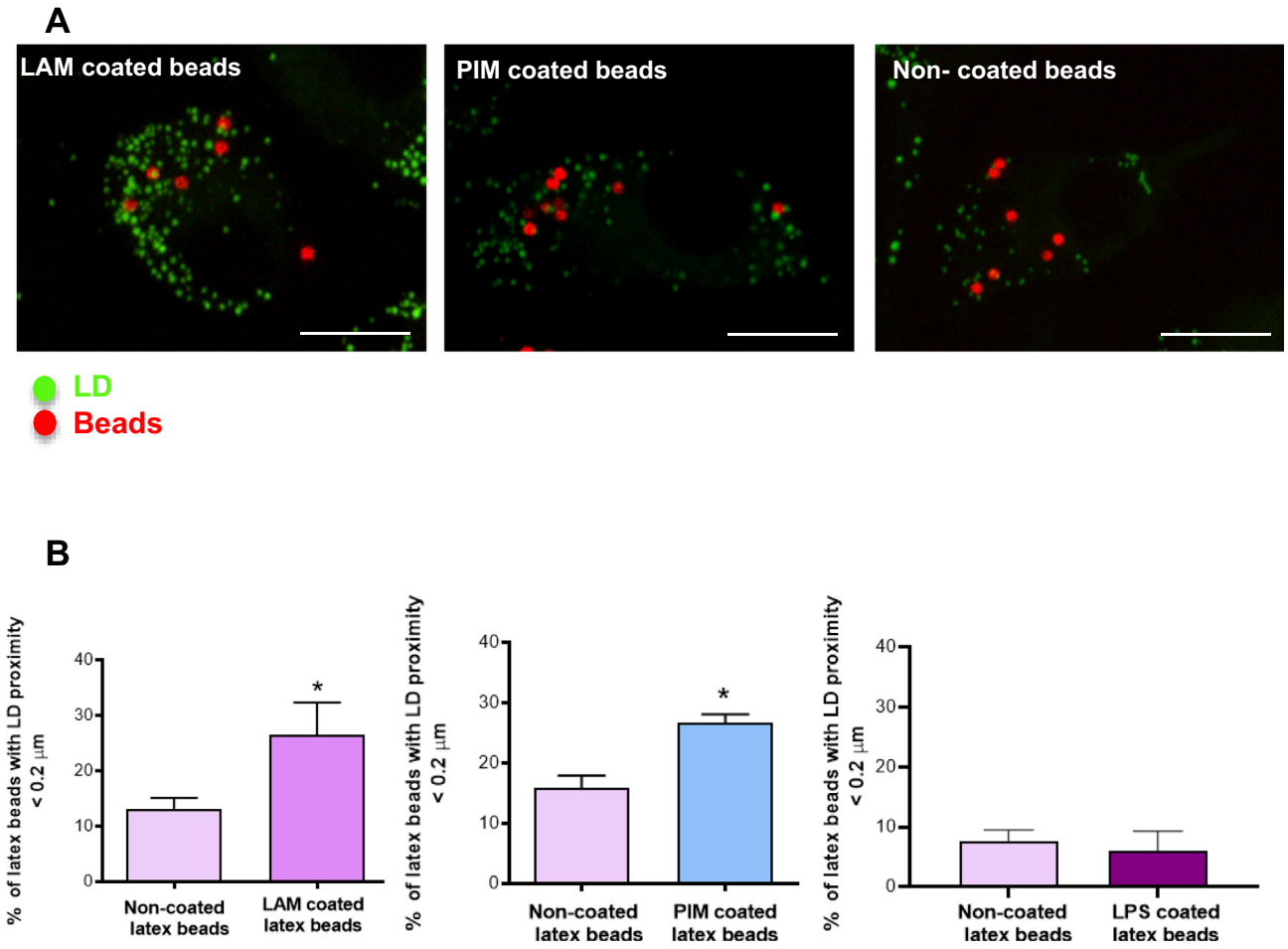

Fig. 3. Role of *M.tb*-derived lipids LAM and PIM on phagosome-lipid droplet (LD) proximity. (A and B) Bone marrow macrophages were loaded with OA (50 uM) for 24 h and then stimulated for 2 h with *M.tb*-derived LAM, PIM, LPS or non-coated fluorescent latex beads (red) (10:1). Lipid droplets were labeled with BODIPY (green) and slides were analyzed by confocal microscopy. (B) Quantification of the distance between beads and LD was performed by using Fiji/ImageJ software from confocal images. In each group, at least 200 cells were analyzed in the total of 10 fields by experiment. Media ± SEM from three to five independent experiments (LAM and PIM). Media ± SEM from 10 fields by each group in from triplicate (LPS). Statistically significant ($p < 0.05$) differences are indicated by *. Bars: 5 µm.

an important role in modulating the host immune response during infection [39,49]. Indeed, LAM and PIM have been implicated in different aspects of the endocytic pathway process. LAM prevents phagosome maturation (through multiple mechanisms) by blocking increases in cytosolic Ca2+ and inhibiting the recruitment of important endocytic proteins [38,50]. Whereas PIM was shown to have a role in stimulating early endosome fusion as a possible mechanism for infecting pathogens to gain access to nutrients [51]. We next evaluated whether the previously observed phagosome-LD association is mediated by mycobacterial cell wall components. For this assay, bone marrow macrophages (BMM) were incubated with fluorescent latex beads that were coated with *M. tuberculosis*-derived LAM, PIM or *E. coli*-derived LPS as previously described [52]. Since an increase in LDs was observed to be induced by LAM-coated latex beads after 2 h (S3), BMM were loaded with oleic acid (OA) 24 h before being stimulated with beads to normalize the number of LD in all groups (Fig. 3A, B and S3). For LD observations, we used BODIPY (493/503) (Fig. 3A). After 2 h of stimulation, we observed phagosomes containing the LAM or PIM coated latex beads in close apposition with BODIPY-labeled LDs, whereas this result was not observed using uncoated latex beads (Fig. 3A and S4) or LPS-coated beads (Fig. 3B). These interactions were quantified by using FIJI/ImageJ to analyze the confocal microscopy images. As observed in Fig. 3B, LAM-coated beads and PIM-coated beads exhibited increased interactions with LDs when compared with uncoated beads (an increase of 102.60% and 67.88%, respectively). From these results, we concluded that LAM and PIM from *M. tuberculosis* are implicated in the interaction between phagosomes and LDs.

3.3. Rab7 but not Rab5 localize to BCG-induced LDs

Rab proteins are small GTPases that act as docking sites for endocytic organelles and are involved in several trafficking and physiological process, such as pathogen clearance and nutrition provision (Reviewed in [53]). Furthermore, Rab7 acquisition by the endosomal compartment has a pivotal role in phagosome maturation. *M. tuberculosis* and *M. bovis* have the ability to retain Rab5 (an early endosome marker) while excluding Rab7 (a late endosome marker) as a mechanism to inhibit phagolysosome biogenesis and increase the survival of bacilli in the host [36,37]. To assess the involvement of LDs with endocytic pathway proteins in this phenomenon, we next examined the localization of Rab5 and Rab7 proteins in macrophages during BCG infection in vivo using immunofluorescence microscopy. Macrophages obtained from BCG-infected mice after 24 h of infection exhibited Rab5 that was close to but not colocalized with LDs labeled with BODIPY, whereas Rab7 was present as a ring surrounding BODIPY-positive LDs (Fig. 4A and B). This result suggests that LDs induced by BCG infection may modulate Rab proteins and could be important to infection progression.

To further understand the function this small GTPase with respect to the observed LD-phagosome association, we investigated the Rab7

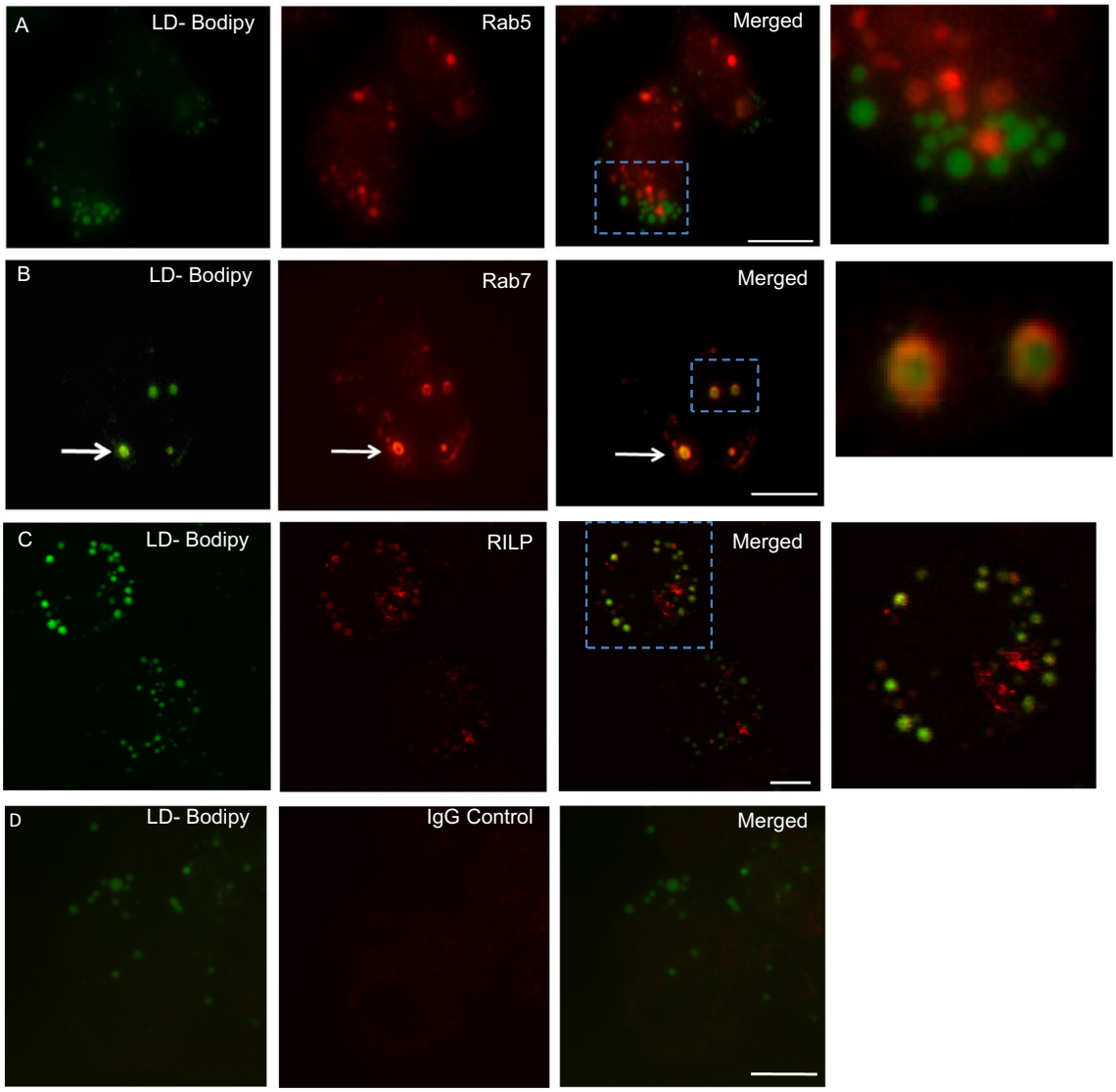

Fig. 4. *M. bovis* BCG induced lipid droplets (LDs) has a specific profile of small GTPases localization. C57/Bl6 mice were i.pl. infected with BCG (5×10^6 CFU/cavity) for 24 or 48 h. Pleural macrophages from infected mice had LD labeled with BODIPY (green) and were immunostained for (A) IgG rabbit anti- Rab5, (B) IgG anti-Rab7 (C) IgG anti-RILP proteins (red). The yellow fluorescence corresponds to colocalization of Rab7 and RILP with LDs. (D) Purified rabbit IgG was used as control. *Right panel*, detail of merged immunostaining. (A, B and D) Slides were analyzed by fluorescent microscopy. Bars: 10 μm. (C) Slides were analyzed by confocal microscopy. (A and B) Data is representative from three independent experiments containing > 100 cells analyzed per group. (C) Data is representative from at least two independent experiments. Bars: 5 μm.

active state via RILP immunofluorescence localization. RILP is an effector of Rab7 protein, and it has been shown that only active Rab7 (GTP bound form) can recruit and bind to the effector Rab-interacting lysosomal protein (RILP) to the phagosomal membrane [32,33]. RILP coordinates the recruitment of the dynein/dynactin motor complex, which in turn promotes the association between late endosomes and lysosomes [32]. To determine if RILP associates with LDs, pleural macrophages from infected C57/Bl6 animals were immunostained with an anti-RILP antibody and incubated with BODIPY to visualize LDs. These cells showed an intense LD accumulation and revealed the presence of RILP colocalized with some, but not all BCG-induced LDs, thus suggesting that Rab7 within LDs is in an active state (Fig. 4C).

3.4. Rab7 colocalizes ultrastructurally with LDs

To investigate the role of Rab7-positive LDs during BCG infection, we next analyzed the localization of this protein via immunogold labeling and TEM. For optimal visualization, after incubating with the primary antibody, the thin sections were incubated with a gold-labeled secondary antibody as previously described [44,48]. In agreement with our previous results, we observed that Rab7 colocalized at the periphery of all LDs (Figs. 5B and S5). By TEM, we analyzed 17 cells showing the entire cell profile and nucleus from the infected group and 37 LDs were observed. All LDs are labeled for Rab7. Furthermore, we examined the significance of the presence of Rab7 in the context of LD-phagosome interactions. Interestingly, we observed an intense accumulation of Rab7 at the contact site with a BCG-infected phagosome (Fig. 5C and D, arrow). Considering the role of Rab proteins in regulating the tethering, fusion and transport of vesicles, these results suggest a role for Rab7 positive LD in the phagosome-LD association.

3.5. Rab7 protein is important for LD-phagosome proximity

The role of Rab7 in the LD-phagosome association was investigated using the Ras superfamily of GTPases GTP/GDP binding antagonist CID1067700. Several studies have demonstrated that CID1067700 acts

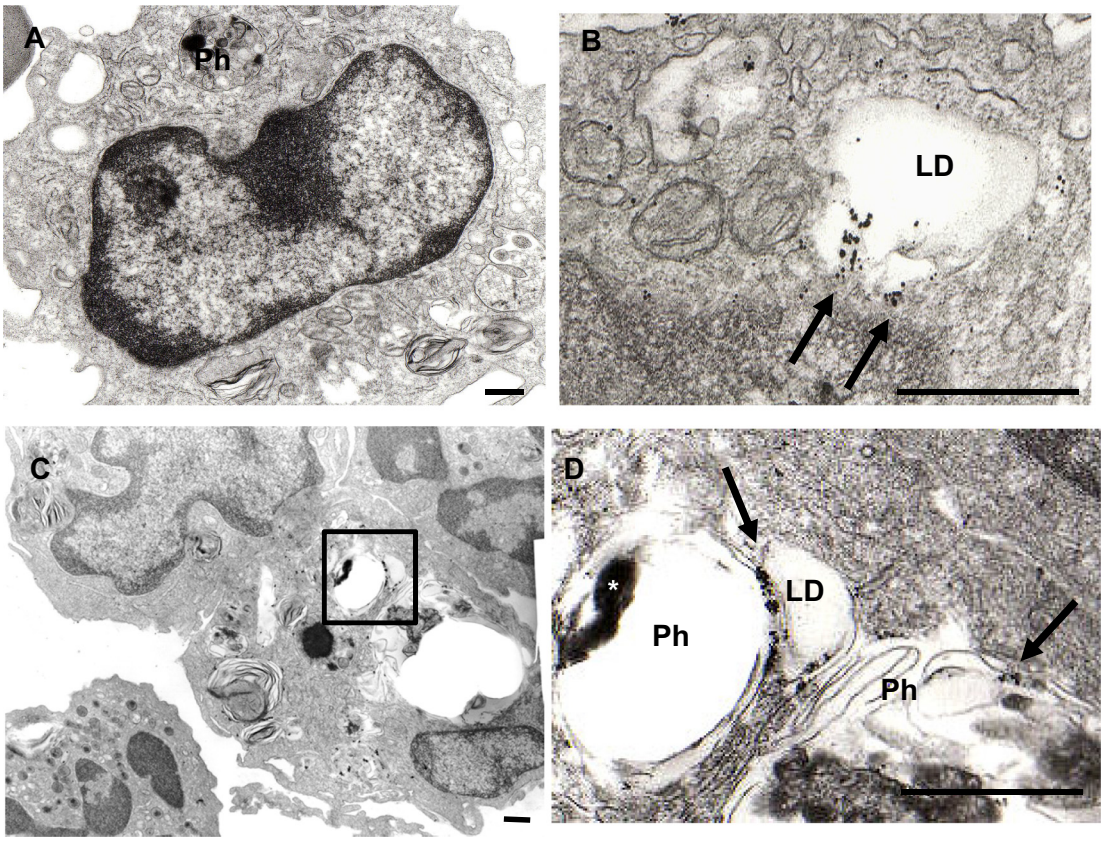

Fig. 5. Rab7 localization on lipid droplets (LDs). C57/Bl6 mice were i.pl. infected with BCG (5×10^6 CFU/cavity) for 24 h. Electron micrographs from pleural macrophages immunogold- labeled for Rab7 at 24 h of infection. (A) Normal rabbit serum was used as negative control, phagosome (Ph), nucleus (N). (B) Presence of Rab7 protein on the surface of LD (*arrow*); and (C and D) between a BCG (*) infected phagosome (Ph) and LD (*arrows and detail*). Representative images of thirteen cells from control and fourteen cells from infected groups in two independent experiments. Bars: 1 μm.

as Rab7 inhibitor by binding in a competitive manner to the nucleotide binding site [54–56]. To elucidate the role of Rab7 in phagosome-LD association, we stimulated OA loaded BMM with non-coated latex beads and LAM-coated latex beads for 2 h followed by a 2 h CID1067700 treatment. A significant decrease in LD-phagosomes association was observed with the 200 nM dose (Fig. 6). In agreement with our previous results showing the presence Rab7 at LDs, these data indicate the involvement of Rab7 in the mechanism by which LD-phagosome association occurs.

4. Discussion

Lipid droplets are multifunctional organelles that have a neutral lipid-rich core that are surrounded by phospholipids and exhibit a cell and stimuli-dependent array of proteins [57–62]. It has been well established that size, number and composition of LDs vary depending on the stimuli and cell type [43,61,63]. During mycobacterial infections, the observed increase in the number of LDs and their relationship with infected phagosomes have been correlated with the success of infection [2,7]. However, the mechanism used by bacilli to mediate this association as well as the role of LDs in the modulation of endocytic proteins during infection remains poorly understood. Here, we present novel data to support that lipid droplet-phagosome interaction occurs through specific and well-regulated mechanisms. Our data suggest that lipid droplet-phagosome interactions are specifically driven by mycobacterial cell wall lipids through Rab7-dependent mechanisms, which enables the exchange of contents between LDs and phagosomes.

In agreement with previews studies, we observed an association between phagosome containing BCG and LDs by confocal microscopy. By immunogold TEM, we also found PLIN2-labeled LD in close apposition with phagosomes (Fig. 1B) strongly suggesting fusion between these two organelles. Moreover, a high number of LDs with morphological changes (irregular surface) were found in the infected group and they were frequently seen within or in contact with phagosomes (Fig. 1C, Fig. S2), indicating that these morphologically affected LDs were directed to phagosomes. The well-described requirement of intracellular pathogenic mycobacteria to use fatty acids and cholesterol as nutrients for growth and persistence support the idea that bacilli must have evolved mechanisms to drive association with LDs during infection [7,11,64]. Moreover, the analyses of TEM showed the presence of bacilli immersed in lipids inside the phagosome. Similar results were observed by Peyron et al. using in vitro human granulomas where peripheral mononuclear blood cells (PBMCs), were infected with *Mtb* and analyzed by TEM [7]. The authors observed LDs in close apposition with phagosomes containing *Mtb* besides the bacilli presence within the core of the LD [7]. This phenomenon could also be observed during other pathogenic mycobacterial infections. *M. leprae* recruitment to LDs was observed in a time-lapse sequence in infected Schwann cells. Moreover, it was possible to observe an LD encasing an infected phagosome as a shield, suggesting a way to protect the bacilli [8].

Moreover, it has been demonstrated that *mycobacterium* can import and metabolize triacylglycerol (TAG) and cholesterol from host LDs [11,12,16,17], demonstrating the utilization of LDs as a nutritional source as an evolutionary advantage. However, accumulation of LDs in host cells has been also suggested to participate in mechanisms to lead to better control of infection by the host through IFN signaling pathway [65] and as a transferable reservoir for antibiotics that enhanced antibacterial efficacy [66].

Curiously, our results are suggestive that lipid trafficking from mycobacteria to host LDs also occur during infection. By utilizing anti-

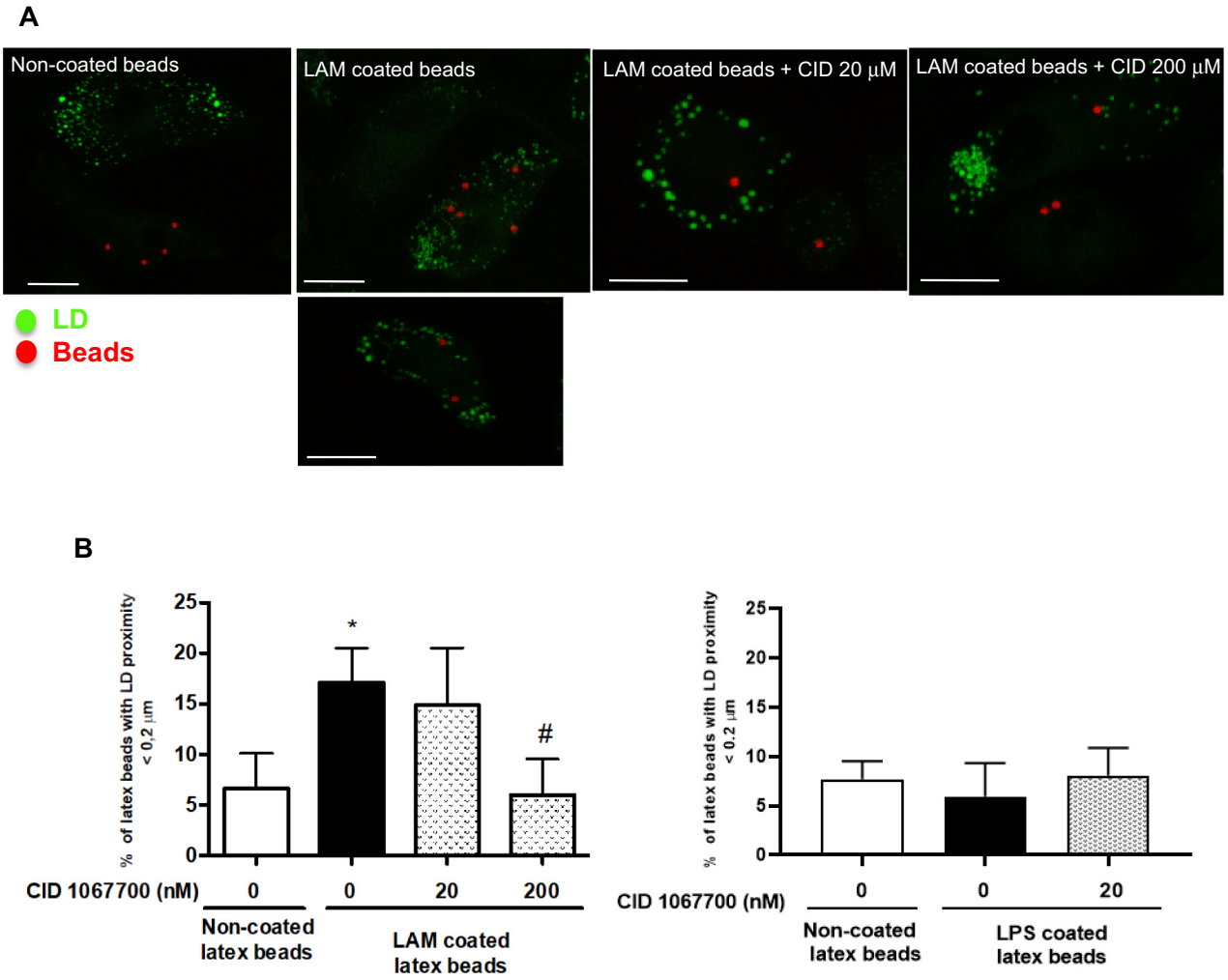

Fig. 6. Rab7 involvement during LD-phagosome proximity. Bone marrow macrophages loaded with OA (50 uM) for 24 h were stimulated for 2 h with LAM and non-coated fluorescent latex beads (red) (10:1). (A) LDs were labeled with BODIPY (green) and slides were analyzed by confocal microscopy. Two representative images for LAM coated beads were presented. (B) Quantification of the distance between latex beads and LD was performed using Fiji/ImageJ software from confocal images. In each group, at least 200 cells were analyzed. Media ± SEM from 10 fields by each group. Data is representative from one of at least two independent experiments (LAM). Media ± SEM from 10 fields by each group in from triplicate (LPS). Statistically significant ($p < 0.05$), differences are indicated by * relative to non-coated latex beads group vs LAM coated latex beads group and # relative to LAM coated latex beads group vs LAM coated latex beads with CID 200 nM group. Bars: 10 μm.

LAM antibodies for immunofluorescence assays, we observed the BCG cell wall glycolipid LAM localizing and staining the bacilli as well as surrouding BODIPY labeled-LD. According to Beatty, cell wall lipids from *M. bovis* BCG are able to leave phagosomes through microvesicles that migrate to different organelles or to uninfected adjacent cells [67]. Further investigations are necessary to elaborate if the observed presence of LAM at LDs occurred due to the microvesicles or from the direct association with a phagosome. In addition, future studies are also needed to determine the significance of LAM in LDs to disease pathogenesis.

Considering the immunomodulatory effects associated with mycobacterial cell wall components, the presence of the glycolipid LAM at LDs may represent a new mechanism by which mycobacteria subvert the host machinery. In this study, we observed that latex beads coated with LAM or with other *M. tb* cell component, PIM were twofold closer to LDs (< 0.2 μm) compared with non-coated latex beads. These results suggest that mycobacterial cell wall components may be responsible for the association between phagosomes and LDs.

The ability of *Mycobacterium* to modulate host macrophages, especially the inhibition of phagosome-lysosome fusion, remains poorly understood. One of the proposed mechanisms for this phenomenon involves LAM interfering in Ca2+ influx in cytosol [50], which inhibits the downstream acquisition of proteins [37,38] and culminates with the impairment of Rab7 recruitment at the phagosome membrane [68]. Here, we showed that the early endosome marker Rab5 does not co-localize with LDs, whereas Rab7 was observed to surround these organelles during *M. bovis* BCG infection in vivo. Moreover, our data indicate the concentration of Rab7 at sites of LD-phagosome interaction. The presence of several Rab proteins in uninfected cells has been described using proteomic analyses of LDs [57,69]. Recently, Saka et al. reported that LDs induced by intracellular *Chlamydia trachomatis* infection exhibited a different protein composition (including lipid metabolism proteins and pathogens proteins) compared to an uninfected control [70]. These observations suggest that mycobacterium infections may modulate the composition of LDs. Collectively, our results raise the possibility that LDs may hijack Rab7 enabling the exchange of contents between LD and phagosomes, and inhibiting the phagosome maturation. Although several mechanisms have been proposed to explain the inhibition of phagosome maturation by mycobacteria, for the first time, we provide a putative role for LDs in this phenomenon.

The function of Rab7 involves the coordination of membrane trafficking, including the docking of vesicles and organelles through the effector protein RILP [33,34]. Since our analyses showed Rab7 accumulation at the site of contact between BCG-infected phagosomes and

LDs, we evaluated whether LD compartmentalized Rab7 was active. RILP (Rab-interacting lysosomal protein), a downstream effector of Rab7, has been considered to be a marker for GTP-Rab7 due to its ability to only interact with active Rab7 [33,71]. In this study, RILP was observed to colocalized with LDs during BCG infection in vivo, suggesting that active form Rab7 associated with LDs during infection. Similar results were described in which HeLa cells were transfected with cDNA for an active and/or inactive form of Rab5. Both types of Rab colocalized with LDs, although only the active form was able to recruit the protein effector EEA1 [72]. In addition, Ozeki and colleagues observed that only the active form of Rab18 colocalizes with LDs in HepG2 cells [73]. In agreement with our results, Schroeder et al. observed the presence of RILP on purified LDs from HuH7 cells [74]. LD dynamics and membrane trafficking were also described in an *S. cerevisiae* model that is related to Rab7-like Ypt7p colocalization [75]. Since RILP has two domains, one that interacts with Rab7 and one that interacts with microtubules through dynein-dynactin motor complex [32], our results raise new possibilities to explain a possible mechanism the association between LDs and infected phagosomes.

The role of Rab7 in LD-phagosome association was investigated using the Ras superfamily GTPases GTP/GDP binding antagonist CID 1067700. Previous studies have shown that CID1067700 acts as Rab7 inhibitor by binding in a competitive manner to the nucleotide binding site [54,56]. To elucidate the role of Rab7 in the association between phagosomes and LDs, BMM were loaded with OA and stimulated with noncoated or LAM-coated latex beads and then treated with CID1067700. A significant decrease in LD-phagosome association was observed with the inhibition of Rab7 by CID1067700, suggesting a role for Rab7 in this association. Accordingly, Rab7 inhibition with siRNA in Hep3B cells was recently shown to impair the recruitment of LDs and multivesicular bodies in a starvation model of autophagy, thus resulting in decreased lipophagy [72]. Of note, Rab7-labeled LDs were recently described during *Toxoplasma gondii* infection [22], suggesting that Rab7 mediated LD-phagosome interaction mechanism described in our study for mycobacterial infection may occur in different infections. Although it is certainly necessary to further investigate the role of Rab7 colocalization with LD during infectious diseases, our results propose a mechanism to explain LD-phagosome association and provide new insights to better understand the mechanism of phagosome maturation impairment.

Transparency document

The Transparency document associated this article can be found, in online version.

CRediT authorship contribution statement

Natalia R. Roque:Investigation, Data curation, Formal analysis, Visualization, Writing - original draft.**Silvia L. Lage**:Investigation, Validation, Writing - review & editing.**Roberta Navarro**:Investigation, Writing - review & editing.**Narayana Fazolini**:Investigation, Validation, Writing - review & editing.**Clarissa M. Maya-Monteiro**:Investigation, Validation, Writing - review & editing.**Jens Rietdorf**:Investigation, Validation, Software, Formal analysis, Writing - review & editing.**Rossana C.N. Melo**:Investigation, Validation, Formal analysis, Funding acquisition, Writing - review & editing.**Heloisa D'Avila**:Conceptualization, Investigation, Validation, Funding acquisition, Supervision, Writing - review & editing.**Patricia T. Bozza**:Conceptualization, Data curation, Funding acquisition, Project administration, Supervision, Visualization, Writing - review & editing.

Declaration of competing interest

The authors declare no competing interests.

Acknowledgments

This work was supported by Conselho Nacional de Desenvolvimento Científico e Tecnológico (CNPq, Brazil), Fundação de Amparo à Pesquisa do Estado do Rio de Janeiro (FAPERJ), Coordenação de Aperfeiçoamento de Pessoal de Nível Superior (CAPES) and Fundação de Amparo à Pesquisa do Estado de Minas Gerais (FAPEMIG, Brazil). The funders had no role in study design, data collection and analysis, decision to publish, or preparation of the manuscript. The following reagents were obtained through BEI Resources, NIAID, NIH: *Mycobacterium tuberculosis*, Strain H37Rv, Purified Lipoarabinomannan (LAM), NR-14848; *Mycobacterium tuberculosis*, Strain H37Rv, Purified Phosphatidylinositol Mannosides 1 & 2 (PIM1,2), NR-14846, Polyclonal antibody LAM (lipoarabinomannan) from H37Rv of *M.tuberculosis* (anti-LAM), NR-13821.

Appendix A. Supplementarty data

References

[1] Y.P. van der Meer-Janssen, J. van Galen, J.J. Batenburg, J.B. Helms, Lipids in host-pathogen interactions: pathogens exploit the complexity of the host cell lipidome, Prog. Lipid Res. 49 (1) (2010) 1–26.
[2] D.G. Russell, P.J. Cardona, M.J. Kim, S. Allain, F. Altare, Foamy macrophages and the progression of the human tuberculosis granuloma, Nat. Immunol. 10 (9) (2009) 943–948.
[3] R.R. Lovewell, C.M. Sassetti, B.C. VanderVen, Chewing the fat: lipid metabolism and homeostasis during M. tuberculosis infection, Curr. Opin. Microbiol. 29 (2016) 30–36.
[4] C. Barisch, T. Soldati, Breaking fat! How mycobacteria and other intracellular pathogens manipulate host lipid droplets, Biochimie 141 (2017) 54–61.
[5] F.S. Pereira-Dutra, L. Teixeira, M.F. de Souza Costa, P.T. Bozza, Fat, fight, and beyond: The multiple roles of lipid droplets in infections and inflammation, J. Leukoc. Biol. 106 (3) (2019) 563–580, https://doi.org/10.1002/JLB.4MR0119-035R.
[6] H. D'Avila, R.C. Melo, G.G. Parreira, E. Werneck-Barroso, H.C. Castro Faria Neto, P.T. Bozza, Mycobacterium bovis BCG induces TLR 2-mediated formation of lipid bodies: intracellular domains for eicosanoid synthesis in vivo, Journal of Immunology 176 (2006) 3087–3097.
[7] P. Peyron, J. Vaubourgeix, Y. Poquet, F. Levillain, C. Botanch, F. Bardou, M. Daffe, J.F. Emile, B. Marchou, P.J. Cardona, C. de Chastellier, F. Altare, Foamy macrophages from tuberculous patients' granulomas constitute a nutrient-rich reservoir for M. tuberculosis persistence, Plos Pathog 4 (11) (2008) e1000204.
[8] K.A. Mattos, F.A. Lara, V.G. Oliveira, L.S. Rodrigues, H. D'Avila, R.C. Melo, P.P. Manso, E.N. Sarno, P.T. Bozza, M.C. Pessolani, Modulation of lipid droplets by Mycobacterium leprae in Schwann cells: a putative mechanism for host lipid acquisition and bacterial survival in phagosomes, Cell. Microbiol. 13 (2) (2011) 259–273.
[9] P.E. Almeida, A.B. Carneiro, A.R. Silva, P.T. Bozza, PPARgamma expression and function in mycobacterial infection: roles in lipid metabolism, immunity, and bacterial killing, PPAR Res. 2012 (2012) 383829.
[10] M.V. Rajaram, M.N. Brooks, J.D. Morris, J.B. Torrelles, A.K. Azad, L.S. Schlesinger, Mycobacterium tuberculosis activates human macrophage peroxisome proliferator-activated receptor gamma linking mannose receptor recognition to regulation of immune responses, J. Immunol. 185 (2) (2010) 929–942.
[11] J. Daniel, H. Maamar, C. Deb, T.D. Sirakova, P.E. Kolattukudy, Mycobacterium tuberculosis uses host triacylglycerol to accumulate lipid droplets and acquires a dormancy-like phenotype in lipid-loaded macrophages, PLoS Pathog. 7 (6) (2011) e1002093.
[12] K.A. Mattos, V.C. Oliveira, M. Berredo-Pinho, J.J. Amaral, L.C. Antunes, R.C. Melo, C.C. Acosta, D.F. Moura, R. Olmo, J. Han, P.S. Rosa, P.E. Almeida, B.B. Finlay, C.H. Borchers, E.N. Sarno, P.T. Bozza, G.C. Atella, M.C. Pessolani, Mycobacterium leprae intracellular survival relies on cholesterol accumulation in infected macrophages: a potential target for new drugs for leprosy treatment, Cell. Microbiol. 16 (6) (2014) 797–815.
[13] H. D'Avila, N.R. Roque, R.M. Cardoso, H.C. Castro-Faria-Neto, R.C. Melo, P.T. Bozza, Neutrophils recruited to the site of Mycobacterium bovis BCG infection undergo apoptosis and modulate lipid body biogenesis and prostaglandin E production by macrophages, Cell. Microbiol. 10 (12) (2008) 2589–2604.
[14] P.E. Almeida, A.R. Silva, C.M. Maya-Monteiro, D. Torocsik, H. D'Avila, B. Dezso, K.G. Magalhaes, H.C. Castro-Faria-Neto, L. Nagy, P.T. Bozza, Mycobacterium bovis bacillus Calmette-Guerin infection induces TLR2-dependent peroxisome proliferator-activated receptor gamma expression and activation: functions in

inflammation, lipid metabolism, and pathogenesis, J. Immunol. 183 (2) (2009) 1337–1345.
[15] J. Rangel Moreno, I. Estrada Garcia, M. De La Luz Garcia Hernandez, D. Aguilar Leon, R. Marquez, R. Hernandez Pando, The role of prostaglandin E2 in the immunopathogenesis of experimental pulmonary tuberculosis, Immunology 106 (2) (2002) 257–266.
[16] C. Barisch, T. Soldati, Mycobacterium marinum degrades both triacylglycerols and phospholipids from its dictyostelium host to synthesise its own triacylglycerols and generate lipid inclusions, PLoS Pathog. 13 (1) (2017) e1006095.
[17] E.J. Munoz-Elias, J.D. McKinney, Mycobacterium tuberculosis isocitrate lyases 1 and 2 are jointly required for in vivo growth and virulence, Nat. Med. 11 (6) (2005) 638–644.
[18] R.C. Melo, A.M. Dvorak, Lipid body-phagosome interaction in macrophages during infectious diseases: host defense or pathogen survival strategy? PLoS Pathog. 8 (7) (2012) e1002729.
[19] J.L. Cocchiaro, Y. Kumar, E.R. Fischer, T. Hackstadt, R.H. Valdivia, Cytoplasmic lipid droplets are translocated into the lumen of the Chlamydia trachomatis parasitophorous vacuole, Proc. Natl. Acad. Sci. U. S. A. 105 (27) (2008) 9379–9384.
[20] A.M. Dvorak, H.F. Dvorak, S.P. Peters, E.S. Shulman, D.W. MacGlashan Jr., K. Pyne, V.S. Harvey, S.J. Galli, L.M. Lichtenstein, Lipid bodies: cytoplasmic organelles important to arachidonate metabolism in macrophages and mast cells, J. Immunol. 131 (6) (1983) 2965–2976.
[21] R.C. Melo, H. D'Avila, D.L. Fabrino, P.E. Almeida, P.T. Bozza, Macrophage lipid body induction by Chagas disease in vivo: putative intracellular domains for eicosanoid formation during infection, Tissue Cell 35 (1) (2003) 59–67.
[22] S.J. Nolan, J.D. Romano, I. Coppens, Host lipid droplets: an important source of lipids salvaged by the intracellular parasite Toxoplasma gondii, PLoS Pathog. 13 (6) (2017) e1006362.
[23] N.E. Rodriguez, R.D. Lockard, E.A. Turcotte, T. Araujo-Santos, P.T. Bozza, V.M. Borges, M.E. Wilson, Lipid bodies accumulation in Leishmania infantum-infected C57BL/6 macrophages, Parasite Immunol. 39 (8) (2017).
[24] A.F. Gomes, K.G. Magalhaes, R.M. Rodrigues, L. de Carvalho, R. Molinaro, P.T. Bozza, H.S. Barbosa, Toxoplasma Gondii-skeletal Muscle Cells Interaction Increases Lipid Droplet Biogenesis and Positively Modulates the Production of IL-12, IFN-g and PGE(2), Parasite Vector 7, (2014) 47.
[25] J.A. Armstrong, P.D. Hart, Response of cultured macrophages to Mycobacterium tuberculosis, with observations on fusion of lysosomes with phagosomes, J. Exp. Med. 134 (3 Pt 1) (1971) 713–740.
[26] S.L. Baltierra-Uribe, J. Garcia-Vasquez Mde, N.S. Castrejon-Jimenez, M.P. Estrella-Pinon, J. Luna-Herrera, B.E. Garcia-Perez, Mycobacteria entry and trafficking into endothelial cells, Can. J. Microbiol. 60 (9) (2014) 569–577.
[27] J. Callaghan, S. Nixon, C. Bucci, B.H. Toh, H. Stenmark, Direct interaction of EEA1 with Rab5b, Eur. J. Biochem. 265 (1) (1999) 361–366.
[28] M. Desjardins, L.A. Huber, R.G. Parton, G. Griffiths, Biogenesis of phagolysosomes proceeds through a sequential series of interactions with the endocytic apparatus, J. Cell Biol. 124 (5) (1994) 677–688.
[29] M. Desjardins, Biogenesis of phagolysosomes: the 'kiss and run' hypothesis, Trends Cell Biol. 5 (5) (1995) 183–186.
[30] J. Rink, E. Ghigo, Y. Kalaidzidis, M. Zerial, Rab conversion as a mechanism of progression from early to late endosomes, Cell 122 (5) (2005) 735–749.
[31] O.V. Vieira, C. Bucci, R.E. Harrison, W.S. Trimble, L. Lanzetti, J. Gruenberg, A.D. Schreiber, P.D. Stahl, S. Grinstein, Modulation of Rab5 and Rab7 recruitment to phagosomes by phosphatidylinositol 3-kinase, Mol. Cell. Biol. 23 (7) (2003) 2501–2514.
[32] I. Jordens, M. Fernandez-Borja, M. Marsman, S. Dusseljee, L. Janssen, J. Calafat, H. Janssen, R. Wubbolts, J. Neefjes, The Rab7 effector protein RILP controls lysosomal transport by inducing the recruitment of dynein-dynactin motors, Curr. Biol. 11 (21) (2001) 1680–1685.
[33] G. Cantalupo, P. Alifano, V. Roberti, C.B. Bruni, C. Bucci, Rab-interacting lysosomal protein (RILP): the Rab7 effector required for transport to lysosomes, EMBO J. 20 (4) (2001) 683–693.
[34] R.E. Harrison, C. Bucci, O.V. Vieira, T.A. Schroer, S. Grinstein, Phagosomes fuse with late endosomes and/or lysosomes by extension of membrane protrusions along microtubules: role of Rab7 and RILP, Mol. Cell. Biol. 23 (18) (2003) 6494–6506.
[35] A. Koul, T. Herget, B. Klebl, A. Ullrich, Interplay between mycobacteria and host signalling pathways, Nat Rev Microbiol 2 (3) (2004) 189–202.
[36] L.E. Via, D. Deretic, R.J. Ulmer, N.S. Hibler, L.A. Huber, V. Deretic, Arrest of mycobacterial phagosome maturation is caused by a block in vesicle fusion between stages controlled by rab5 and rab7, J. Biol. Chem. 272 (20) (1997) 13326–13331.
[37] R.A. Fratti, J.M. Backer, J. Gruenberg, S. Corvera, V. Deretic, Role of phosphatidylinositol 3-kinase and Rab5 effectors in phagosomal biogenesis and mycobacterial phagosome maturation arrest, J. Cell Biol. 154 (3) (2001) 631–644.
[38] I. Vergne, J. Chua, V. Deretic, Tuberculosis toxin blocking phagosome maturation inhibits a novel Ca2+/calmodulin-PI3K hVPS34 cascade, J. Exp. Med. 198 (4) (2003) 653–659.
[39] I. Vergne, J. Chua, H.H. Lee, M. Lucas, J. Belisle, V. Deretic, Mechanism of phagolysosome biogenesis block by viable Mycobacterium tuberculosis, Proc. Natl. Acad. Sci. U. S. A. 102 (11) (2005) 4033–4038.
[40] S. Axelrod, H. Oschkinat, J. Enders, B. Schlegel, V. Brinkmann, S.H. Kaufmann, A. Haas, U.E. Schaible, Delay of phagosome maturation by a mycobacterial lipid is reversed by nitric oxide, Cell. Microbiol. 10 (7) (2008) 1530–1545.
[41] D. Wong, H. Bach, J. Sun, Z. Hmama, Y. Av-Gay, Mycobacterium tuberculosis protein tyrosine phosphatase (PtpA) excludes host vacuolar-H+-ATPase to inhibit phagosome acidification, Proc. Natl. Acad. Sci. U. S. A. 108 (48) (2011) 19371–19376.
[42] R.C. Melo, L.A. Spencer, S.A. Perez, J.S. Neves, S.P. Bafford, E.S. Morgan, A.M. Dvorak, P.F. Weller, Vesicle-mediated secretion of human eosinophil granule-derived major basic protein, Lab. Investig. 89 (7) (2009) 769–781.
[43] F.F. Dias, V.C. Zarantonello, G.G. Parreira, H. Chiarini-Garcia, R.C. Melo, The intriguing ultrastructure of lipid body organelles within activated macrophages, Microsc. Microanal. 20 (3) (2014) 869–878.
[44] R.C. Melo, E. Morgan, R. Monahan-Earley, A.M. Dvorak, P.F. Weller, Pre-embedding immunogold labeling to optimize protein localization at subcellular compartments and membrane microdomains of leukocytes, Nat. Protoc. 9 (10) (2014) 2382–2394.
[45] K. Tanigawa, K. Suzuki, K. Nakamura, T. Akama, A. Kawashima, H. Wu, M. Hayashi, S. Takahashi, S. Ikuyama, T. Ito, N. Ishii, Expression of adipose differentiation-related protein (ADRP) and perilipin in macrophages infected with Mycobacterium leprae, FEMS Microbiol. Lett. 289 (1) (2008) 72–79.
[46] D.G. Russell, Phagosomes, fatty acids and tuberculosis, Nat. Cell Biol. 5 (9) (2003) 776–778.
[47] K.A. Mattos, V.G. Oliveira, H. D'Avila, L.S. Rodrigues, R.O. Pinheiro, E.N. Sarno, M.C. Pessolani, P.T. Bozza, TLR6-driven lipid droplets in Mycobacterium leprae-infected Schwann cells: immunoinflammatory platforms associated with bacterial persistence, J. Immunol. 187 (5) (2011) 2548–2558.
[48] R.C. Melo, Depletion of immune effector cells induces myocardial damage in the acute experimental Trypanosoma cruzi infection: ultrastructural study in rats, Tissue Cell 31 (3) (1999) 281–290.
[49] J.B. Torrelles, L.S. Schlesinger, Diversity in Mycobacterium tuberculosis mannosylated cell wall determinants impacts adaptation to the host, Tuberculosis (Edinb) 90 (2) (2010) 84–93.
[50] R.A. Fratti, J. Chua, I. Vergne, V. Deretic, Mycobacterium tuberculosis glycosylated phosphatidylinositol causes phagosome maturation arrest, Proc. Natl. Acad. Sci. U. S. A. 100 (9) (2003) 5437–5442.
[51] I. Vergne, R.A. Fratti, P.J. Hill, J. Chua, J. Belisle, V. Deretic, Mycobacterium tuberculosis phagosome maturation arrest: mycobacterial phosphatidylinositol analog phosphatidylinositol mannoside stimulates early endosomal fusion, Mol. Biol. Cell 15 (2) (2004) 751–760.
[52] L.S. Schlesinger, S.R. Hull, T.M. Kaufman, Binding of the terminal mannosyl units of lipoarabinomannan from a virulent strain of Mycobacterium tuberculosis to human macrophages, J. Immunol. 152 (8) (1994) 4070–4079.
[53] M. Zhang, L. Chen, S. Wang, T. Wang, Rab7: roles in membrane trafficking and disease, Biosci. Rep. 29 (3) (2009) 193–209.
[54] J.O. Agola, L. Hong, Z. Surviladze, O. Ursu, A. Waller, J.J. Strouse, D.S. Simpson, C.E. Schroeder, T.I. Oprea, J.E. Golden, J. Aube, T. Buranda, L.A. Sklar, A. Wandinger-Ness, A competitive nucleotide binding inhibitor: in vitro characterization of Rab7 GTPase inhibition, ACS Chem. Biol. 7 (6) (2012) 1095–1108.
[55] T. Lam, D.V. Kulp, R. Wang, Z. Lou, J. Taylor, C.E. Rivera, H. Yan, Q. Zhang, Z. Wang, H. Zan, D.N. Ivanov, G. Zhong, P. Casali, Z. Xu, Small molecule inhibition of Rab7 impairs B cell class switching and plasma cell survival to dampen the autoantibody response in murine lupus, J. Immunol. 197 (10) (2016) 3792–3805.
[56] L. Hong, Y. Guo, S. BasuRay, J.O. Agola, E. Romero, D.S. Simpson, C.E. Schroeder, P. Simons, A. Waller, M. Garcia, M. Carter, O. Ursu, K. Gouveia, J.E. Golden, J. Aube, A. Wandinger-Ness, L.A. Sklar, A pan-GTPase inhibitor as a molecular probe, PLoS One 10 (8) (2015) e0134317.
[57] B.D. Hodges, C.C. Wu, Proteomic insights into an expanded cellular role for cytoplasmic lipid droplets, J. Lipid Res. 51 (2) (2010) 262–273.
[58] A. Lass, R. Zimmermann, G. Haemmerle, M. Riederer, G. Schoiswohl, M. Schweiger, P. Kienesberger, J.G. Strauss, G. Gorkiewicz, R. Zechner, Adipose triglyceride lipase-mediated lipolysis of cellular fat stores is activated by CGI-58 and defective in Chanarin-Dorfman syndrome, Cell Metab. 3 (5) (2006) 309–319.
[59] R. Bartz, J.K. Zehmer, M. Zhu, Y. Chen, G. Serrero, Y. Zhao, P. Liu, Dynamic activity of lipid droplets: protein phosphorylation and GTP-mediated protein translocation, J. Proteome Res. 6 (8) (2007) 3256–3265.
[60] H.C. Wan, R.C. Melo, Z. Jin, A.M. Dvorak, P.F. Weller, Roles and origins of leukocyte lipid bodies: proteomic and ultrastructural studies, FASEB J. 21 (1) (2007) 167–178.
[61] P.T. Bozza, K.G. Magalhaes, P.F. Weller, Leukocyte lipid bodies - biogenesis and functions in inflammation, Biochim. Biophys. Acta 1791 (6) (2009) 540–551.
[62] A. Pol, S.P. Gross, R.G. Parton, Review: biogenesis of the multifunctional lipid droplet: lipids, proteins, and sites, J. Cell Biol. 204 (5) (2014) 635–646.
[63] H.A. Saka, R. Valdivia, Emerging roles for lipid droplets in immunity and host-pathogen interactions, Annu. Rev. Cell Dev. Biol. 28 (2012) 411–437.
[64] A.K. Pandey, C.M. Sassetti, Mycobacterial persistence requires the utilization of host cholesterol, Proc. Natl. Acad. Sci. U. S. A. 105 (11) (2008) 4376–4380.
[65] M. Knight, J. Braverman, K. Asfaha, K. Gronert, S. Stanley, Lipid droplet formation in Mycobacterium tuberculosis infected macrophages requires IFN-gamma/HIF-1alpha signaling and supports host defense, PLoS Pathog. 14 (1) (2018) e1006874.
[66] D.J. Greenwood, M.S. Dos Santos, S. Huang, M.R.G. Russell, L.M. Collinson, J.I. MacRae, A. West, H. Jiang, M.G. Gutierrez, Subcellular antibiotic visualization reveals a dynamic drug reservoir in infected macrophages, Science 364 (6447) (2019) 1279–1282.
[67] W.L. Beatty, E.R. Rhoades, H.J. Ullrich, D. Chatterjee, J.E. Heuser, D.G. Russell, Trafficking and release of mycobacterial lipids from infected macrophages, Traffic 1 (3) (2000) 235–247.
[68] I. Vergne, M. Gilleron, J. Nigou, Manipulation of the endocytic pathway and phagocyte functions by Mycobacterium tuberculosis lipoarabinomannan, Front. Cell. Infect. Microbiol. 4 (2015) 187.
[69] N. Krahmer, M. Hilger, N. Kory, F. Wilfling, G. Stoehr, M. Mann, R.V. Farese Jr., T.C. Walther, Protein correlation profiles identify lipid droplet proteins with high confidence, Mol. Cell. Proteomics 12 (5) (2013) 1115–1126.
[70] H.A. Saka, J.W. Thompson, Y.S. Chen, L.G. Dubois, J.T. Haas, A. Moseley,

R.H. Valdivia, Chlamydia trachomatis infection leads to defined alterations to the lipid droplet proteome in epithelial cells, PLoS One 10 (4) (2015) e0124630.
[71] M. Wu, T. Wang, E. Loh, W. Hong, H. Song, Structural basis for recruitment of RILP by small GTPase Rab7, EMBO J. 24 (8) (2005) 1491–1501.
[72] P. Liu, R. Bartz, J.K. Zehmer, Y.S. Ying, M. Zhu, G. Serrero, R.G. Anderson, Rab-regulated interaction of early endosomes with lipid droplets, Biochim. Biophys. Acta 1773 (6) (2007) 784–793.
[73] S. Ozeki, J. Cheng, K. Tauchi-Sato, N. Hatano, H. Taniguchi, T. Fujimoto, Rab18 localizes to lipid droplets and induces their close apposition to the endoplasmic reticulum-derived membrane, J. Cell Sci. 118 (Pt 12) (2005) 2601–2611.
[74] B. Schroeder, R.J. Schulze, S.G. Weller, A.C. Sletten, C.A. Casey, M.A. McNiven, The small GTPase Rab7 as a central regulator of hepatocellular lipophagy, Hepatology 61 (6) (2015) 1896–1907.
[75] I. Bouchez, M. Pouteaux, M. Canonge, M. Genet, T. Chardot, A. Guillot, M. Froissard, Regulation of lipid droplet dynamics in Saccharomyces cerevisiae depends on the Rab7-like Ypt7p, HOPS complex and V1-ATPase, Biol Open 4 (7) (2015) 764–775.